

Received May 14, 2018, accepted June 22, 2018, date of publication July 9, 2018, date of current version July 30, 2018.

Digital Object Identifier 10.1109/ACCESS.2018.2854225

# High Gain and Wideband High Dense Dielectric Patch Antenna Using FSS Superstrate for Millimeter-Wave Applications

MUFTAH ASAADI<sup>ID</sup>, (Student Member, IEEE), ISLAM AFIFI<sup>ID</sup>, (Student Member, IEEE),  
AND ABDEL-RAZIK SEBAK, (Fellow, IEEE)

Electrical and Computer Engineering Department, Concordia University, Montréal, QC H4B 1R6, Canada

Corresponding author: Muftah Asaadi (m\_assadi@encs.concordia.ca)

**ABSTRACT** Gain and bandwidth enhancement of low profile, linearly polarized square dense dielectric patch antennas using a frequency selective surface (FSS) superstrate layer is proposed. A high dense dielectric patch antenna is utilized as a radiating element instead of a metallic patch in order to gain several significant advantages, including low profile, wide bandwidth, and high radiation efficiency. The implemented antenna is excited by an aperture-coupled feeding technique. The antenna gain is enhanced by using a highly reflective FSS superstrate layer, realizing an antenna gain enhancement of 11 dBi. The implemented antenna acquired a measured gain of about 17.78 dBi at 28 GHz with a 9% bandwidth and radiation efficiency of 90%. The bandwidth of the proposed antenna is improved by using a unit cell printed on two sides, as it provides a positive phase gradient over the desired frequency range. The antenna impedance bandwidth is broadened and the measured impedance matching  $S_{11}$  exhibited a 15.54% instead of 9% bandwidth while maintaining a high-gain characteristic of about 15.4 dBi. The implemented antenna presents a solid radiation performance with good agreement between the measured and simulation results. For some attractive advantages such as low profile, low cost, lightweight, small size, and ease of implementation, the proposed antenna is a very good candidate for millimeter-wave wireless communications.

**INDEX TERMS** Millimeter-wave antennas, high gain, broad bandwidth, high dense dielectric (DD) patch, superstrate, FSS, 5G applications.

## I. INTRODUCTION

Future wireless communication systems will need wider bandwidth, higher speeds, and low latency. The millimeter wave band has therefore been selected for its ability to provide all of the next generation's requirements. High-gain wideband antennas capable of working in the millimeter-wave spectrum are also required [1]. Due to the high attenuation in the atmosphere and the low output power of millimeter-wave solid state sources, millimeter-wave applications require antennas with high gain in order to compensate for different losses [2].

Dielectric resonators have been used as dielectric resonator antennas (DRAs) since the 1980s. Recently, a thin high dense dielectric (DD) patch with high permittivity was used to replace a metallic patch, thereby realizing some attractive characteristics including wide bandwidth and high radiation efficiency [3]–[6]. In [6], a perforated superstrate was used to

enhance the antenna gain as well as to improve the bandwidth. However, the antenna radiated elements were  $2 \times 2$  DD patch arrays. In [7], a highly reflective metamaterial surface was used as a superstrate over the antenna patch, with a gain of about 12.5 dBi, and 3 dB gain bandwidth of about 10%. The linearly polarized antennas reported in [8] and [9] offer low gain and they use bulky multi-FSS layers. In [10], three layers of FSS superstrate were applied over a microstrip patch antenna in order to enhance the antenna performance, realizing an antenna gain of about 14.2 dBi with low radiation efficiency. A high-gain circularly polarized dielectric resonator antenna is reported in [11]. It uses an FSS superstrate to enhance the antenna gain, achieving a high gain of about 15.5 dBi.

An essential drawback of electromagnetic band gap (EBG) resonator antennas is the narrow frequency bandwidth due to their naturally narrowband resonant cavity [12].

Several methods to improve the bandwidth have been published. A wide-band reconfigurable partially reflective surface (PRS) antenna was implemented in [13] to function throughout a broad frequency range. In [14], the bandwidth of an EBG resonator antenna is improved up to 13.2 % by using a slot antenna array. However, the antenna structures and their fabrication in both [13] and [14] are complicated, which is not a good match with the simplicity of the EBG resonator antenna. Based on the analysis in [15], a PRS with a reflection phase resembles the optimum phase where the reflection phase is proportional to the frequency can be used to produce a broadband EBG resonator cavity antenna. That finding led to PRSs with positive reflection phase gradients being implemented using two dielectric layers separated by an air gap to produce wideband EBG resonator antennas [16]. Another approach utilized a dual-layer PRS to provide a positive phase gradient with a 2-D different FSS unit cell, the unit cell composed of two different FSSs [17]. However, the 3 dB gain bandwidth was 12.2 %.

In this work, a highly reflective FSS superstrate layer is placed above a square dense dielectric (DD) patch antenna to enhance the antenna gain. The metallic patch is replaced with a high dense dielectric patch with relative permittivity of 82. The high dense patch antenna is excited using a coupling slot etched off the common ground plane. A set of highly reflective unit cells is put over the DD patch as a superstrate layer to act as a lens to improve the antenna gain. Another set of 7×7 unit cells with the positive reflection phase (PRP) feature is also applied over the same DD patch antenna to broaden the antenna’s bandwidth. The proposed antenna offers high gain, high radiation efficiency, and wide frequency bandwidth. The air gap between the square DD patch and the FSS layer with an identical set of FSS unit cells is optimized to enhance the antenna gain and to improve the antenna impedance matching. These presented antennas are a suitable candidate for 5G applications.

The paper is organized as follows. The antenna structure and the two unit cells are described next, in section II, followed by their performances indicated in both the measured and simulated results. The work is then summarized and concluded in section III.

**II. ANTENNA DESIGN**

The configuration of the DD patch antenna with the FSS superstrate is shown in Fig. 1. The DD patch is designed on a Rogers RT/duroid 6002 ( $\epsilon_r = 2.94$  and  $\tan\delta = 0.0009$ ) substrate. The bottom substrate is a Rogers RT 3010 ( $\epsilon_r=10.2$  and  $\tan\delta = 0.0023$ ). Both substrates are the same thickness ( $h_1 = h_2$ ). The slot, which is used to excite the DD patch, is etched in the ground plane of a microstrip line. A 50  $\Omega$  microstrip line is printed on the bottom side of the bottom substrate with dimensions of  $L_f$  and  $W_f$ . An array of uniform 7×7 unit cells is implemented on the bottom side of the superstrate dielectric layer, a Rogers RT/duroid 5880 ( $\epsilon_r = 2.2$  and  $\tan\delta = 0.0009$ ). The FSS superstrate is covered

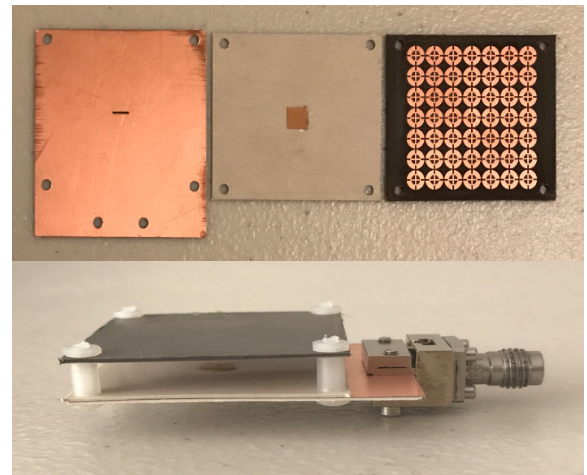
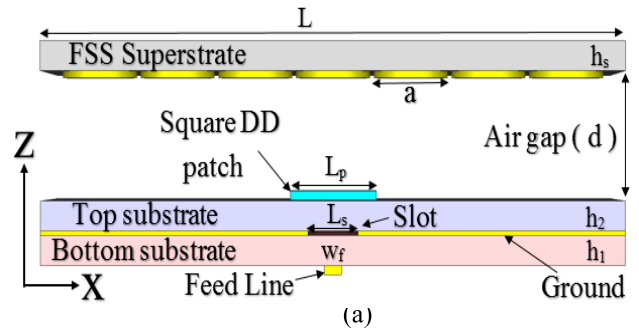


**FIGURE 1. Geometry of the proposed antenna: (a) side view, (b) photographs of the antenna prototype.**

the DD patch antenna at an air gap height  $d$ . The optimized parameters are listed in Table 1.

**TABLE 1. Antenna parameters.**

Parameters	Value (mm)
$L_p$	4.5
$H_p$	0.15
$L$	32
$W$	32
$h_1$	0.508
$h_2$	0.508
$L_f$	16
$W_f$	0.39
$L_s$	3.571
$W_s$	0.2
$h_s$	0.787
$d$	5.35

**A. HIGHLY REFLECTIVE UNIT CELL DESIGN**

The implemented unit cell is designed and studied. The geometry of the FSS utilized as the superstrate layer is depicted in Fig. 2. It is implemented on a Rogers RT/duroid 5880 ( $\epsilon_r = 2.2$  and  $\tan\delta = 0.0009$ ) with thickness  $h=0.787$  mm. The final dimensions of the proposed unit cell are:  $a = 4$  mm,

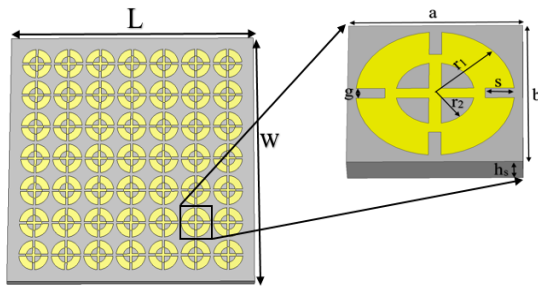


FIGURE 2. Bottom side of the FSS superstrate, and the geometry of the proposed unit cell.

$b = 4 \text{ mm}$ ,  $h_s = 0.787 \text{ mm}$ ,  $r_1 = 1.9 \text{ mm}$ ,  $r_2 = 0.94 \text{ mm}$ ,  $s = 0.77 \text{ mm}$ , and  $g = 0.3 \text{ mm}$ . The FSS unit cell’s performance versus frequency is illustrated in Fig. 3. These results indicate that the DD patch antenna gain can be enhanced if the FSS reflection magnitude increases to unity. Therefore, a flat reflection phase and high reflection magnitude are targeted for the FSS superstrate. The magnitude of the reflection coefficient  $|\Gamma_{FSS}|$  at  $(\theta = 0)$  for a normal incident wave can be utilized to calculate the directivity  $D$  [18]:

$$D = 10 \log \frac{1 + |\Gamma_{FSS}|}{1 - |\Gamma_{FSS}|} \quad (1)$$

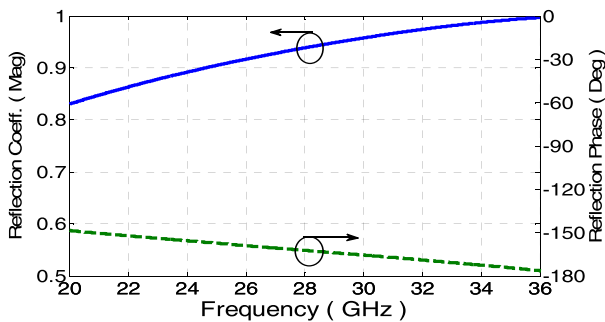


FIGURE 3. Performance of the proposed unit cell.

Equation (1) shows that the directivity increases significantly as magnitude of the reflection coefficient increases. Therefore, in order to achieve high gain performance, a high reflection magnitude should be achieved within the design frequency. The superstrate of a set of the highly reflective FSS unit cells acts as a lens, allowing a high reflection magnitude to be achieved inside the antenna’s resonant cavity and thus a high gain for the antenna is obtained.

To validate the simulated results, a DD patch antenna with a highly reflective superstrate was fabricated and measured. The implemented antenna was studied and simulated using the CST full-wave electromagnetic simulation tool. Fig 4 shows the measured and the simulated return losses of the proposed antenna, with an impedance matching bandwidth of around 9%. It can be observed that there is a quite discrepancy between the measured and the simulated results,

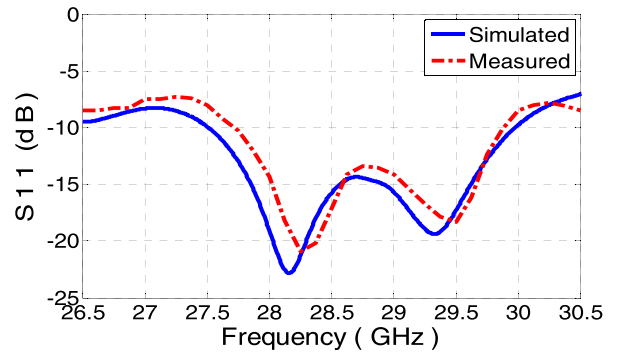


FIGURE 4. Reflection coefficient of the DD patch antenna with a positive reflection phase unit cell.

even though they do follow the same pattern. The relative permittivity for all dielectric layers are given at 10 GHz in the manufacture’s data sheet. Accordingly, the value of  $\epsilon_r$  is altered at the MMW bands, and may cause a shift in the design frequency [6], [19]. High measured gain of about 17.78 dBi at 28 GHz, and radiation efficiency of almost 90 % are shown in Fig 5.

Fig. 6 shows the E- and H-plane simulated and measured radiation patterns of the proposed square DD patch antenna with highly reflective superstrate at 28 GHz and at 29 GHz, indicating that the antenna provides good radiation patterns and side lobe levels (SLLs). The SLLs are below  $-15 \text{ dB}$  at 28 GHz (design frequency), and then increase a little bit as the frequency is increased.

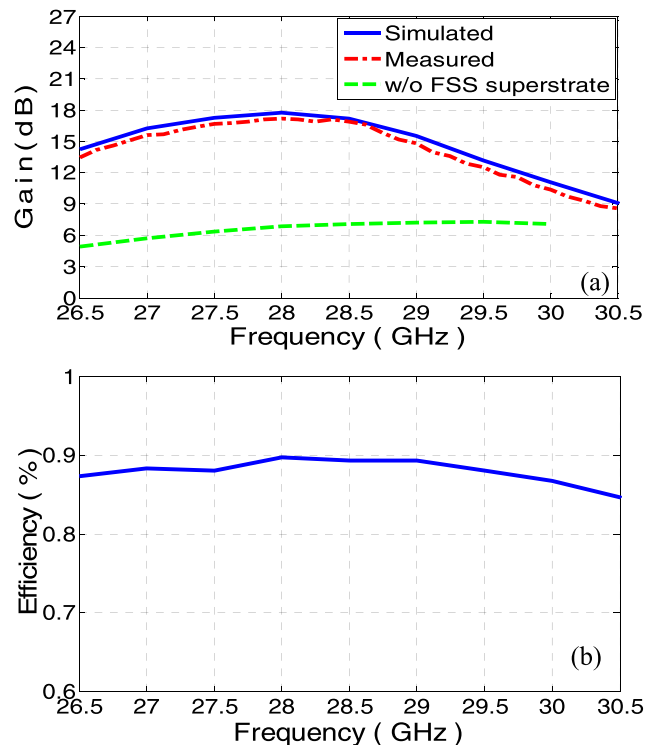


FIGURE 5. Simulated and measured gain (a), and simulated radiation efficiency (b) of the proposed antenna.

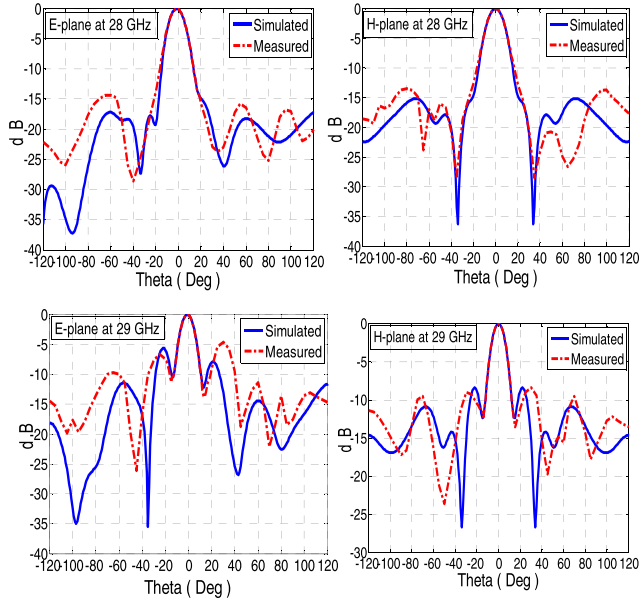


FIGURE 6. E- and H-plane radiation patterns of the proposed antenna for different frequencies.

**B. DESIGN OF UNIT CELL WITH POSITIVE PHASE GRADIENT**

Since the DD patch antenna with a highly reflective FSS in part A provided only a 9 % bandwidth, a new unit cell is proposed to broaden the antenna bandwidth while keeping the high gain. This section presents the design procedure of a unit cell that provides a positive reflection phase gradient to be utilized as a superstrate of the high DD patch antenna. In general, a partially reflective surface (PRS) can be defined as the periodic arrays of metallic unit cells printed on either one or both sides of a dielectric material. The FSS superstrate is usually applied at a distance  $d$  of about half a wavelength (the air gap) above the antenna source; the high DD patch antenna in this design. Multiple reflections are generated between the PRS surface and the ground plane. These lead to constructive interference and enhance the gain of the antenna towards the broadside direction when the air gap between the FSS superstrate and the ground plane is equal to [17]:

$$d = \frac{\lambda}{2} \left( \frac{\phi}{2\pi} + 0.5 \right) + N \frac{\lambda}{2} \tag{2}$$

where  $\Phi$  is the reflection phase of the PRS,  $\lambda$  is the free space wavelength, and  $N$  is the mode order. Equation (2) can be rewritten in the following form to give the optimum phase where the PRS and the ground plane are assumed to be infinite and the air gap distance  $d=5.7$  mm:

$$\phi = \frac{4\pi d}{c} f - (2N - 1) \pi \tag{3}$$

Equation (3) reveals how a higher gain can be achieved by obtaining a positive reflection phase gradient  $\Phi$  in terms of the frequency over the entire desired operating frequency. Both of the unit cells are designed and simulated using

the CST full-wave electromagnetic simulation tool. A unit cell boundary conditions are applied to the four side walls of a unit cell, as shown in Fig. 7(c). Normal incidence is applied and the incident electric field is polarized along the direction of the bottom strip.

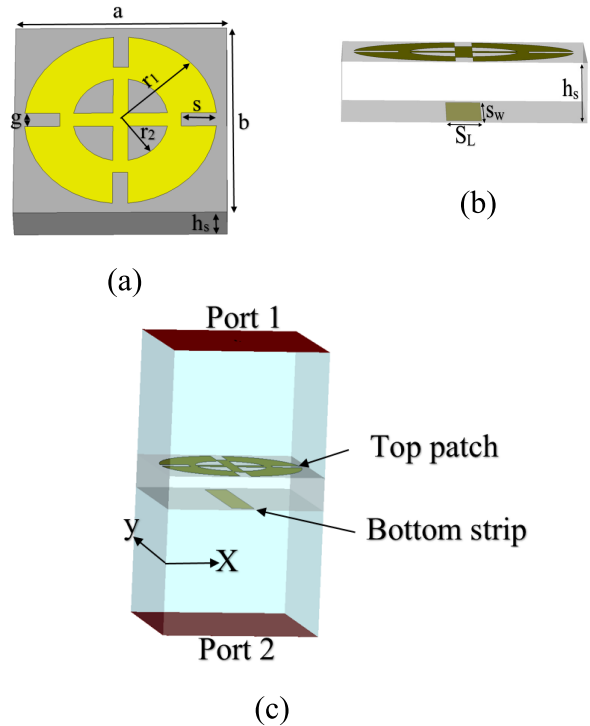


FIGURE 7. Geometry of the proposed unit cell: (a) top view, (b) side view, (c) Characterization model of the unit cell.

In this part, the unit cell is designed to generate a positive phase gradient. To achieve this, a two-sided printed unit cell is designed, as shown in Fig 7. The bottom side of the unit cell is almost the same as that of the unit cell utilized in part A. The top part is the strip line designed to be parallel with the E-field to create a positive reflection phase gradient. The positive reflection phase unit cell is printed on a Rogers RT/duroid 5880 ( $\epsilon_r = 2.2$  and  $\tan\delta = 0.0009$ ) substrate with a thickness of 0.31 mil. The unit cell has a periodicity of  $p = 3.78$  mm. A full-wave electromagnetic simulation tool (CST Microwave Studio) was used to design the proposed unit cell. After optimization, the final dimensions of the two-sided printed unit cell are obtained as:  $a = 3.78$  mm,  $b = 3.78$  mm,  $h_s = 0.787$  mm,  $r_1 = 1.71$  mm,  $r_2 = 0.85$  mm,  $s = 0.69$  mm,  $g = 0.27$  mm,  $S_w = 0.54$  mm,  $S_L = 3.15$  mm for the bottom. Fig. 8 illustrates the phase and magnitude of the reflection coefficient of the unit cell when the plane wave is incident normally on the bottom side of the unit cell.

As shown in Fig. 8, the proposed unit cell produces a phase that closely resembles the optimum phase in its positive gradient within the operating frequency. A parametric study was conducted to evaluate the effect of certain design parameters, such as  $S_L$  and  $S_w$ , on the unit cell performance.



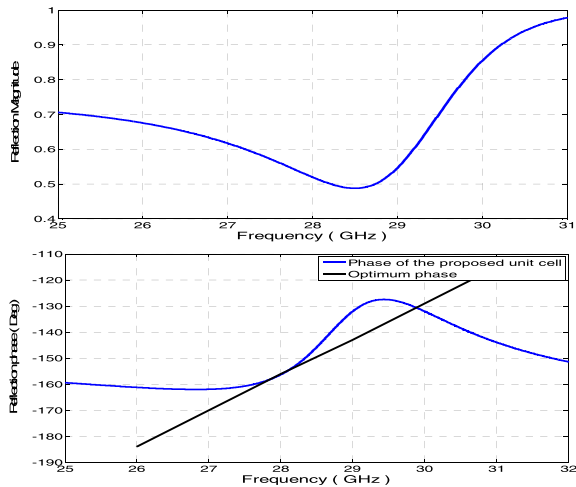


FIGURE 8. The magnitude and reflection phase of the proposed unit cell.

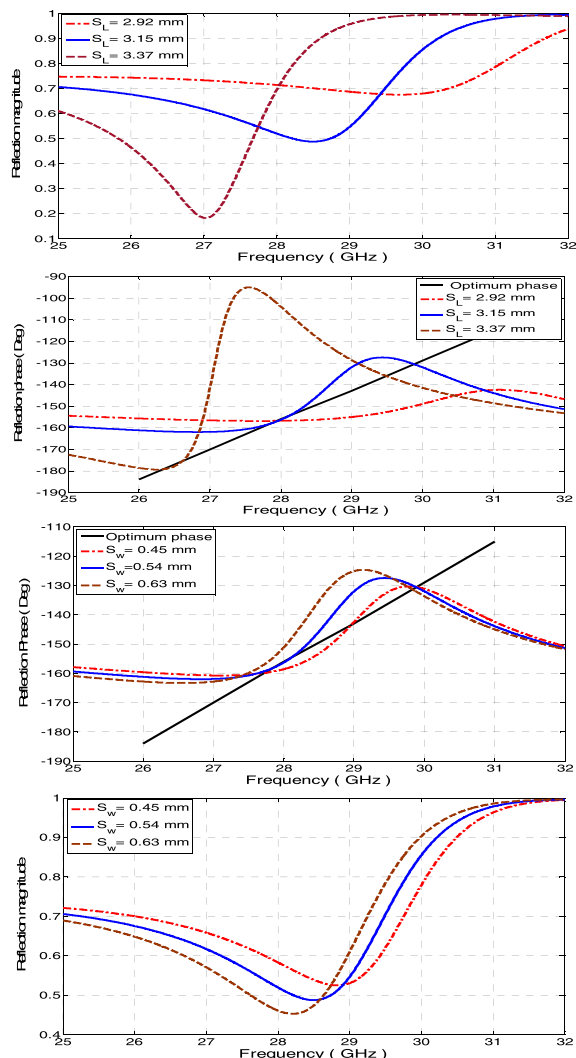


FIGURE 9. Effect of  $S_L$  and  $S_w$  parameters on unit cell performance.

Fig. 9 clearly shows that both  $S_L$  and  $S_w$  have an impact on the phase gradient and on the reflection coefficient. Both the reflection magnitude and phase of the proposed unit cell are

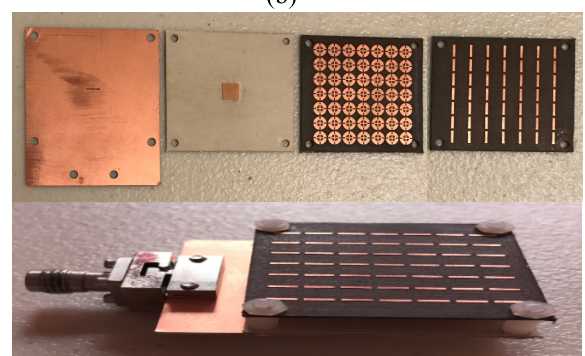
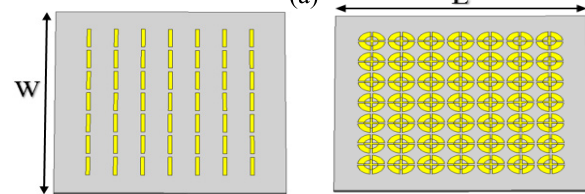
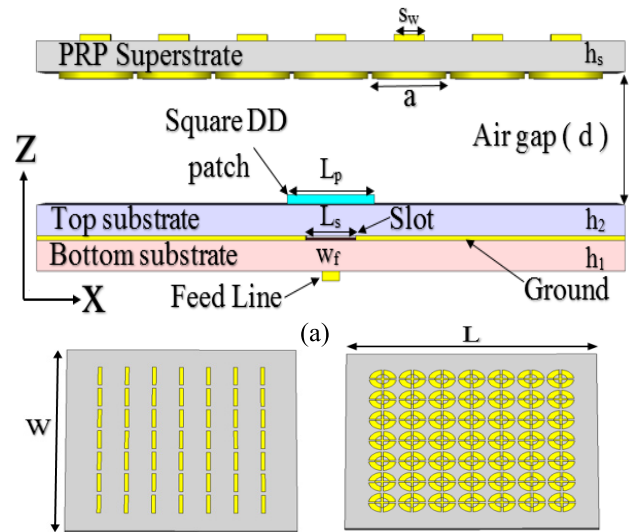


FIGURE 10. Geometry of the proposed antenna with a PRP unit cells: (a) side view, (b) top and bottom of the superstrate, (c) photographs of the antenna prototype.

shifted toward lower frequencies as  $S_L$  is increased, and vice versa. As  $S_L$  increases, the reflection magnitude decreases, moving away from the designed frequency band. This results in a low gain antenna with a disrupted bandwidth, where high reflection magnitude with positive phase gradient is required to achieve a high gain antenna with wide bandwidth. The parameter  $S_w$  has little impact on the unit cell's performance.

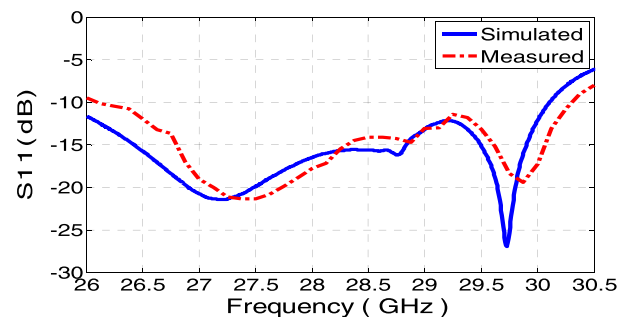


FIGURE 11. Reflection coefficient of the DD patch antenna with a positive reflection phase superstrate.

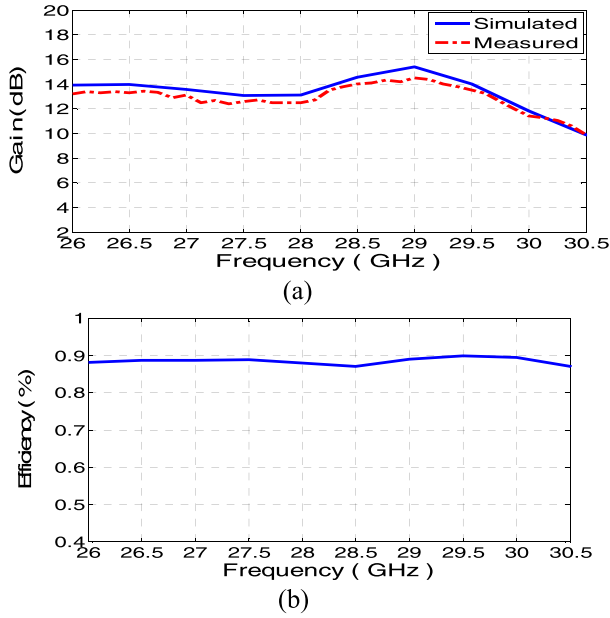


FIGURE 12. Gain (a) and radiation efficiency (b) of the DD patch antenna with a positive phase gradient unit cell.

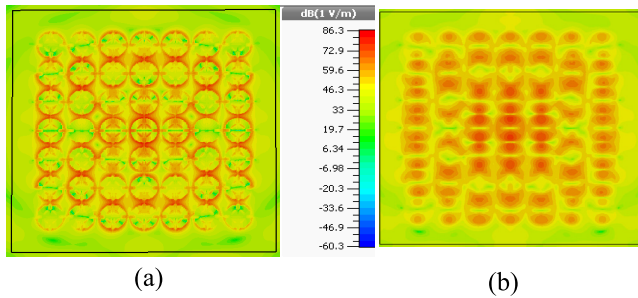


FIGURE 13. E-field distribution of the DD patch antenna with a positive phase at 28 GHz: Bottom of the superstrate (a), and top of the superstrate (b).

To verify the simulated results, a square DD patch with an FSS superstrate based on the positive reflection phase gradient was fabricated and tested as depicted in Fig. 10. The simulated and measured return losses of the proposed antenna are shown in Fig. 11. They exhibit a 15.54 % wider bandwidth compared to the 9 % bandwidth for the DD patch with a highly reflective unit cell used in part A. The simulated and measured gain together with the simulated radiation efficiency of the proposed antenna are plotted in Fig 12.

The results indicate that a good agreement between the measured and the simulated antenna gain was achieved. An almost 14 dBi gain was obtained over the operating band, where the maximum gain is about 15.4 dBi at 29 GHz. The simulated radiation efficiency of the antenna is about 90 % over the whole bandwidth. There are some antenna parameters that could affect the antenna performance, such as the air gap  $d$ . It is found that  $d$  has the significant effect on the antenna resonance, and less effect on the antenna gain. As  $d$  increases the resonance frequency is shifted down and

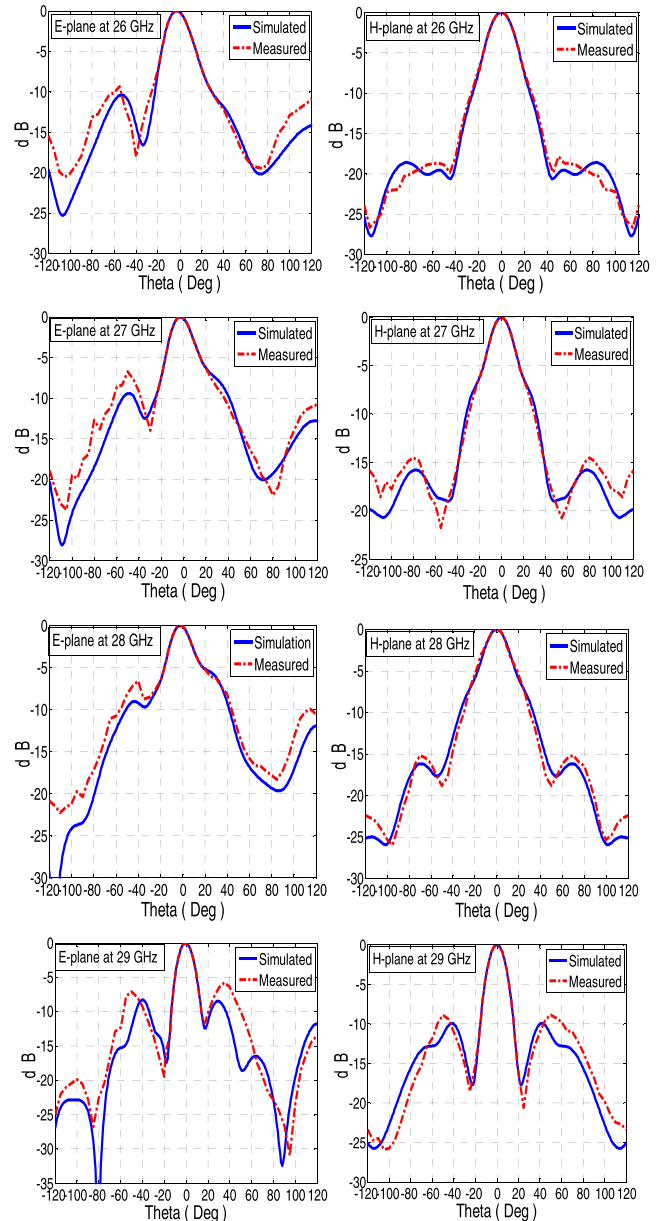


FIGURE 14. E- and H-plane radiation pattern of the DD patch with a positive phase superstrate for different frequencies.

vice versa. The E- field distribution of DD patch antenna with a positive phase gradient superstrate is illustrated in Fig. 13.

Fig. 14 shows the simulated and measured radiation patterns of the proposed square DD patch antenna with a positive phase gradient superstrate at 26, 27, 28, and 29 GHz. A good agreement is obtained between the measured and simulated results. Therefore, the side lobe levels can be assumed to be better (overall) at all frequencies within the antenna band, except for the E-plane at 29 GHz and 30 GHz (not shown here). These exceptions are due to the multiple reflections that become greater at higher frequencies.

Table 2 compares the proposed designs to several published works, highlighting the improved performance of the

**TABLE 2. Performance comparison of our proposed design with designs in the literature.**

Ref. N°	Freq. (GHz)	Max. Gain (dBi)	3dB Gain BW %	Substrate Type	Antenna element
[11]	30	15	10	FSS ( one layer)	DRA
[17]	60	16	12.2	FSS( Two layers)	Slot antenna
[20]	13.7	16.3	10.9	FSS (Three layers)	Slot antenna
This work	<b>28</b>	<b>17.78</b>	<b>9</b>	FSS(highly reflective, one layer)	DD patch Antenna
	<b>28</b>	<b>15.4</b>	<b>15.5</b>	FSS (Positive phase gradient, one layer)	DD patch Antenna

proposed antenna. The proposed antenna provides a good performance in terms of gain and in 3 dB gain bandwidth compared to other relevant works.

### III. CONCLUSION

A linearly polarized low-profile square dense dielectric (DD) patch antenna with gain and bandwidth enhancement using a frequency selective surface (FSS) superstrate layer is proposed. Two different FSS superstrates are utilized to enhance the gain and bandwidth. A superstrate of a set of highly reflective planar unit cells was designed and placed above the DD patch antenna by almost a half wavelength to enhance the antenna gain, realizing an enhancement of 11 dBi. The implemented antenna acquired a measured gain of about 17.78 dBi at 28 GHz with a 9 % bandwidth, and radiation efficiency of about 90 %. In addition, a superstrate layer of an array of reflection phase unit cells was designed to improve the bandwidth of the proposed antenna. Using this superstrate resulted in a 6 % enhancement of the antenna bandwidth with almost a 15.4 dBi gain. Simulated and measured results for S11 show a 15.54 % impedance matching bandwidth.

### REFERENCES

- [1] H. Vettikalladi, O. Lafond, and M. Himdi, "High-efficient and high-gain superstrate antenna for 60-GHz indoor communication," *IEEE Antennas Wireless Propag. Lett.*, vol. 8, pp. 1422–1425, 2009.
- [2] A. Vosoogh, P. S. Kildal, and V. Vassilev, "Wideband and high-gain corporate-fed gap waveguide slot array antenna with ETSI class II radiation pattern in V-band," *IEEE Trans. Antennas Propag.*, vol. 65, no. 4, pp. 1823–1831, Apr. 2017.
- [3] H. W. Lai, K.-M. Luk, and K. W. Leung, "Dense dielectric patch antenna—A new kind of low-profile antenna element for wireless communications," *IEEE Trans. Antennas Propag.*, vol. 61, no. 8, pp. 4239–4245, Aug. 2013.
- [4] A. A. Kishk, A. Ittipiboon, Y. M. M. Antar, and M. Cuhaci, "Slot excitation of the dielectric disk radiator," *IEEE Trans. Antennas Propag.*, vol. 43, no. 2, pp. 198–201, Feb. 1995.
- [5] Y. Li and K.-M. Luk, "Wideband perforated dense dielectric patch antenna array for millimeter-wave applications," *IEEE Trans. Antennas Propag.*, vol. 63, no. 8, pp. 3780–3786, Aug. 2015.
- [6] M. Asaadi and A. Sebak, "Gain and bandwidth enhancement of  $2 \times 2$  square dense dielectric patch antenna array using a holey superstrate," *IEEE Antennas Wireless Propag. Lett.*, vol. 16, pp. 1808–1811, 2017.

- [7] A. K. Singh, M. P. Abegaonkar, and S. K. Koul, "High-gain and high-aperture-efficiency cavity resonator antenna using metamaterial superstrate," *IEEE Antennas Wireless Propag. Lett.*, vol. 16, pp. 2388–2391, 2017.
- [8] M. J. Al-Hasan, T. A. Denidni, and A. R. Sebak, "Millimeter-wave EBG-based aperture-coupled dielectric resonator antenna," *IEEE Trans. Antennas Propag.*, vol. 61, no. 8, pp. 4354–4357, Aug. 2013.
- [9] Y. Jia, Y. Liu, H. Wang, K. Li, and S. Gane, "Low-RCS, high-gain, and wideband mushroom antenna," *IEEE Antennas Wireless Propag. Lett.*, vol. 14, pp. 277–280, 2015.
- [10] B. P. Chacko, G. Augustin, and T. A. Denidni, "FPC antennas: C-band point-to-point communication systems," *IEEE Antennas Propag. Mag.*, vol. 58, no. 1, pp. 56–64, Feb. 2016.
- [11] M. Akbari, S. Gupta, M. Farahani, A. R. Sebak, and T. A. Denidni, "Gain enhancement of circularly polarized dielectric resonator antenna based on FSS superstrate for MMW applications," *IEEE Trans. Antennas Propag.*, vol. 64, no. 12, pp. 5542–5546, Dec. 2016.
- [12] Y. Ge, K. P. Esselle, and T. S. Bird, "The use of simple thin partially reflective surfaces with positive reflection phase gradients to design wideband, low-profile EBG resonator antennas," *IEEE Trans. Antennas Propag.*, vol. 60, no. 2, pp. 743–750, Feb. 2012.
- [13] A. R. Weily, T. S. Bird, and Y. J. Guo, "A reconfigurable high-gain partially reflecting surface antenna," *IEEE Trans. Antennas Propag.*, vol. 56, no. 11, pp. 3382–3390, Nov. 2008.
- [14] A. R. Weily, K. P. Esselle, T. S. Bird, and B. C. Sanders, "Dual resonator 1-D EBG antenna with slot array feed for improved radiation bandwidth," *IET Microw., Antennas Propag.*, vol. 1, no. 1, pp. 198–203, Feb. 2007.
- [15] A. P. Feresidis and J. C. Vardaxoglou, "High gain planar antenna using optimised partially reflective surfaces," *IEE Proc.-Microw., Antennas Propag.*, vol. 148, no. 6, pp. 345–350, Dec. 2001.
- [16] C. Mateo-Segura, A. P. Feresidis, and G. Goussetis, "Highly directive 2-D leaky wave antennas based on double-layer meta-surfaces," in *Proc. 4th Eur. Conf. Antennas Propag.*, Barcelona, Spain, 2010, pp. 1–5.
- [17] H. Attia, M. L. Abdelghani, and T. A. Denidni, "Wideband and high-gain millimeter-wave antenna based on FSS Fabry–Pérot cavity," *IEEE Trans. Antennas Propag.*, vol. 65, no. 10, pp. 5589–5594, Oct. 2017.
- [18] A. Foroozesh and L. Shafai, "Investigation into the effects of the patch-type FSS superstrate on the high-gain cavity resonance antenna design," *IEEE Trans. Antennas Propag.*, vol. 58, no. 2, pp. 258–270, Feb. 2010.
- [19] A. Elboushi, O. Haraz, and A. Sebak, "High gain circularly polarized slot-coupled antenna for millimeter wave applications," *Microw. Opt. Technol. Lett.*, vol. 56, no. 11, pp. 2522–2526, 2014.
- [20] K. Konstantinidis, A. P. Feresidis, and P. S. Hall, "Broadband sub-wavelength profile high-gain antennas based on multi-layer metasurfaces," *IEEE Trans. Antennas Propag.*, vol. 63, no. 1, pp. 423–427, Jan. 2015.



**MUFTAH ASAADI** (S'16) received the B.Sc. degree in electronics and communications engineering from the College of Electronic Technology, Baniwaleed, Libya, in 2001, and the M.Sc. degree in electrical and computer engineering from the Libyan Academy, Libya, in 2009. He is currently pursuing the Ph.D. degree in electrical and computer engineering with Concordia University, Montréal, QC, Canada. From 2010 to 2012, he was a Lecturer with the Communication Department, Faculty of Engineering, Baniwaleed University. He was a Teaching Assistant with the Department of Communication Engineering, College of Electronic Technology. His current research interests include analysis and antenna design, high gain millimeter-wave antennas, dielectric resonator antennas, and frequency selective surface.



**ISLAM AFIFI** (S'18) received the B.Sc. degree in electronics and communication engineering and the M.Sc. degree in engineering physics from Cairo University, Cairo, Egypt, in 2009 and 2014, respectively. He is currently pursuing the Ph.D. degree in electrical and computer engineering with Concordia University, Montréal, QC, Canada. He was a Teaching and Research Assistant with the Engineering Mathematics and Physics Department, Cairo University, from 2009 to 2014, where

he was a Senior Teaching Assistant from 2014 to 2016. His research interests are millimeter-wave microwave components and antennas.



**ABDEL-RAZIK SEBAK** (F'10) received the B.Sc. degree (Hons.) in electrical engineering from Cairo University, Cairo, Egypt, in 1976, the B.Sc. degree in applied mathematics from Ain Shams University, Cairo, in 1978, and the M.Eng. and Ph.D. degrees in electrical engineering from the University of Manitoba, Winnipeg, MB, Canada, in 1982 and 1984, respectively. From 1984 to 1986, he was with Canadian Marconi Company, involved in the design of microstrip phased array

antennas. From 1987 to 2002, he was a Professor with the Department of Electronics and Communication Engineering, University of Manitoba. He is currently a Professor with the Department of Electrical and Computer Engineering, Concordia University, Montréal, QC, Canada. His research interests include phased array antennas, millimeter-wave antennas and imaging, computational electromagnetics, and interaction of EM waves with engineered materials and bio electromagnetics. He is a member of the Canadian National Committee of International Union of Radio Science Commission B. He was a recipient of the 2000 and 1992 University of Manitoba Merit Award for outstanding Teaching and Research, the 1994 Rh Award for Outstanding Contributions to Scholarship and Research, and the 1996 Faculty of Engineering Superior. He served as the Chair for the IEEE Canada Awards and Recognition Committee from 2002 to 2004 and the Technical Program Chair for the 2002 IEEE CCECE Conference and the 2006 URSIANTEM Symposium. He is the Technical Program Co-Chair of the 2015 IEEE ICUWB Conference.

• • •